Original Paper

Titanium corrosion in molten glasses

Part 2. Electrochemical study and corrosion mechanisms

Christophe Rapin, Renaud Podor, Sylvain Michon, Patrice Berthod and Stéphane Mathieu

Laboratoire de Chimie du Solide Minéral, Université Henri Poincaré, Nancy I, Vandoeuvre-les-Nancy (France)

In situ electrochemical experiments are carried out to determine the mechanisms of pure titanium corrosion in molten glasses. The corrosion layers formed at the metal/glass interface are systematically reported. The formal potentials of the Ti^{III}/Ti^{II} and Ti^{IV}/Ti^{III} redox couples are respectively positioned at −1.0 V and −0.7 V by coupling square wave voltammetry measurements and polarization of titanium rods. The potential of the B^{III}/B^{0} couple is estimated to be near −1.4 V. The results obtained by immersion tests and electrochemical measurements in glasses are compared. They are consistent in terms of corrosion rate variations and morphology of the corrosion scales. The corrosion mechanisms are described in the form of successive redox reactions between the glass and the substrate followed by diffusion of the formed species into the titanium substrate. It is demonstrated that Ti does not form spontaneously protective scales when immersed in molten glass and that protection can not be reached by either anodic or cathodic polarization.

1. Introduction

Pursuing the study of titanium corrosion in molten glasses of Part I of this work [1], specific in situ electrochemical experiments are carried out using a special device. The aim of this work is to determine the corrosion mechanisms of titanium in molten glasses.

This metal has the ability to incorporate high oxygen contents in solid solution and to form Ti^{II}, Ti^{III} and Ti^{IV} oxides. That is the reason why classical immersion tests in molten glass [1] are coupled with electrochemical techniques (as previously reported by Di Martino et al. [2] for Ni, Fe, Cr and Co behavior in molten glass). The influence of an imposed potential on the material is studied. The results collected are expressed in the form of metal/glass interface morphology, and potentiodynamic or current recordings.

2. Materials

The following materials were used:

Metal rods: Ti, 99.7 % purity (Alfa Aesar) – initial diameter is adjusted to fit with the internal diameter of the mullite-made tubes used for electrochemical experiments.

Glass: The electrochemical measurements are recorded in the G–S glass. Its composition (in wt%) is 64.5 SiO_2, 4.5 B_2O_3, 3.4 Al_2O_3, 16.0 Na_2O, 1.2 K_2O, 7.2 CaO, 3.1 MgO and 0.15 Fe_2O_3.

Received 4 April, revised manuscript 29 September 2003.

Part 1. Immersion tests and corrosion kinetics. Glass Sci. Technol. **77** (2004) no. 1, pp. 36–43.

3. Experimental procedure

3.1 Electrochemical techniques

The apparatus used for this study was extensively described in the literature [2 and 3]. A furnace in which a Pt-10%Rh crucible filled with 1.5 kg of glass is heated to 1050 °C. Four electrodes' tips are immersed in the glass melt. They respectively correspond to:

- two counter electrodes made of platinum (25 x 1 x 10) mm^3,
- an yttria stabilized reference electrode [4 and 5],
- a working electrode. This working electrode is a Pt wire (1 mm diameter) for the glass study and a 5.5 mm diameter Ti rod polished to the 2400 grid SiC paper for metal/glass corrosion studies.

PAR M273 or M263A potentiostats were used to perform the electrochemical measurements. Free potential recording, polarization resistance measurements (Stern-Geary's method), linear polarization, cyclic and square wave voltammetry methods were used when needed. Long lasting free potential recordings were coupled with a polarization resistance determination every two hours. The polarization resistance (R_p) was determined by scanning the potential at a rate of 0.166 mV s^{-1} over the range of $E_c \pm 10$ mV. The scan rate of 0.166 mV s^{-1} was applied for the potentiodynamic scan, recorded from −20 mV versus corrosion poten-

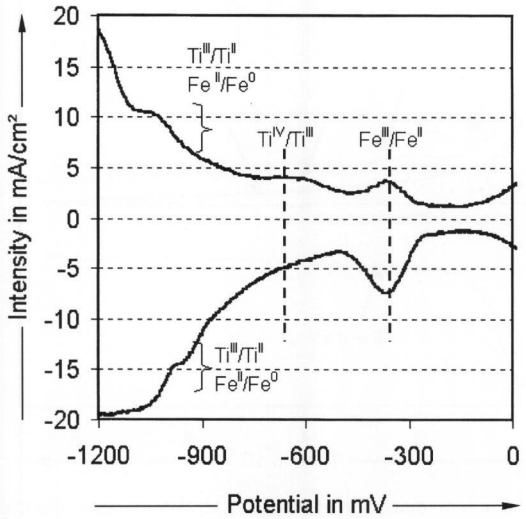

Figure 1. Anodic and cathodic current versus potential curves recorded on Ti-enriched G–S glass by square wave voltammetry.

tial to +700 mV. Anodic and cathodic polarizations were performed by imposing the potential on the titanium rod versus zirconia electrode and recording the current during 24 h. In this study, all the potentials are given versus the yttria stabilized reference electrode.

3.2 Scanning electron microscopy and electron microprobe analysis

The SEM investigations were performed with a Philips XL30 instrument (Philips, Eindhoven (The Netherlands)) using a 15 kV accelerating voltage. The quantitative determinations of the composition of the different phases were made using a CAMECA SX50 electron microprobe (Cameca, Courbevoie (France)). These techniques are extensively described in [1].

4. Results

4.1 Formal potentials of Ti couples

The knowledge of the formal potentials of the titanium couples is a useful tool to interpret titanium reactions in different glass melts. The Ti^{IV}/Ti^{III} formal potential is positioned at −0.860 V by Von der Gönna et al. [6]. A specific electrochemical study was carried out in the G–S glass in order to state this value more precisely and to determine the Ti^{III}/Ti^{II} formal potential. A platinum electrode is introduced into a titanium enriched glass. The classical electrochemical techniques are used to characterize dissolved titanium ions [7 to 9]. Cyclic voltammetry suffers from a poor sensitivity and therefore results are not given here. Anodic and cathodic current-potential curves obtained by square wave voltammetry are reported in figure 1. The Fe^{II}/Fe^0 and Fe^{III}/Fe^{II} characteristic peaks can be noted on these curves at respectively −1.0 V and −0.4 V. These results are in good

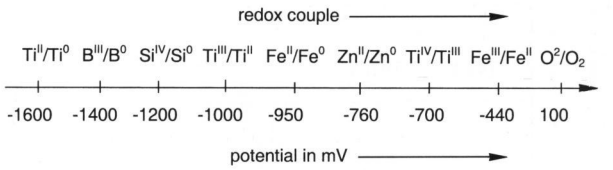

Figure 2. Positioning of the different redox couples encountered in the present study.

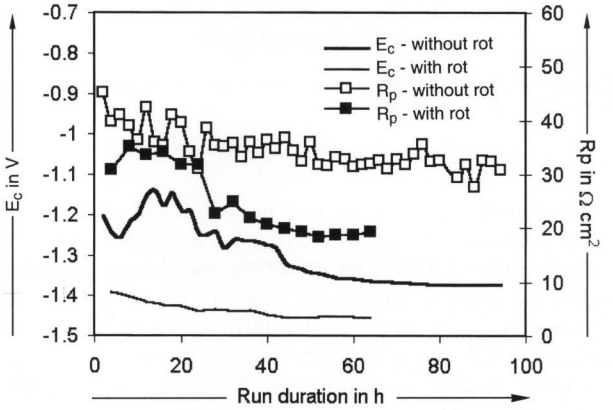

Figure 3. Corrosion potential E_c and polarization resistance R_p measurement of titanium in the G–S glass at T = 1050 °C. rot stands for rotation.

agreement with data previously published [10]. The anodic curve clearly exhibits an additional peak close to −0.7 V that can be assigned to the Ti^{IV}/Ti^{III} system. Considering results reported in the literature [6] and the current value of the peak located at −1.0 V (that is too high to correspond only to the Fe^{II}/Fe^0 system) is allotted to both Fe^{II}/Fe^0 and a titanium system. Taking into account that the Ti^{IV}/Ti^{III} redox couple value is −0.7 V and that the Ti^{II}/Ti^0 redox couple value is lower than −1.2 V (the silica network of the glass is reduced at the titanium contact), the peak observed at −1.0 V can only be attributed to the Ti^{III}/Ti^{II} redox couple. The Ti^{II} species are not necessarily present in the glass as free cations. The redox potentials used to understand the corrosion of titanium are reported in figure 2.

4.2 Free potentials and polarization resistances

The free potentials (E_c) and polarization resistance values (R_p) have been recorded for 96 h in both static and dynamic conditions (figure 3). Titanium equilibrates with glass in a few hours. Both E_c and R_p reach a value that is almost constant with time. The stability of measured values versus time is evidence of the solubility of corrosion products. If these values were not stable, the accumulation of corrosion products at the metal/glass interface would slow down the corrosion rate and therefore an increase in the R_p values would be measured. This result is in good accordance with the observation shown in figures 7a and b of Part 1 [1], where no precipitated phase is present in the glass surrounding the metals. Furthermore, the E_c values that are measured indicate that the oxidation of titanium is mainly due to the reduction of the silicate network.

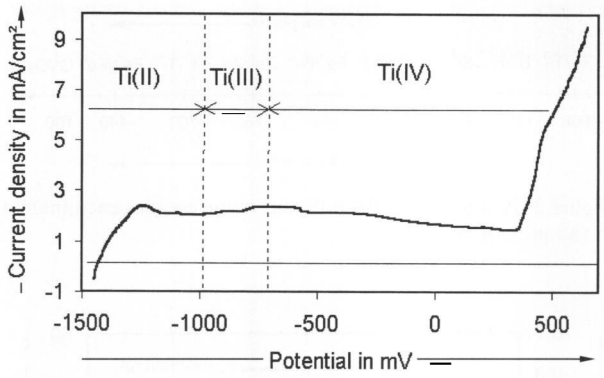

Figure 4. Anodic polarization curve of titanium (scan rate 600 mV/h, T = 1050 °C).

Although values of the free potentials are of the same order of magnitude in both static and dynamic conditions (respectively −1.35 V and −1.45 V), the sample morphologies are different (figures 7a and b in [1]). In static conditions, the corrosion layers that form at the metal/glass interface are well defined and the frontiers between each other are clear. In dynamic conditions, the glass draws the corrosion layers. The thicknesses of the corrosion layers are lowered in comparison with those determined under static conditions. In both cases, the R_p values are low (respectively 35 Ω cm² in static and 20 Ω cm² in dynamic conditions) and characteristic of an active corrosion.

4.3 Polarization curve of titanium

The anodic polarization curve of titanium recorded from E_c to +700 mV is reported in figure 4. This curve exhibits a small anodic peak (near −1250 mV) with a critical intensity of 2.5 mA/cm² followed by a pseudo passivation plateau. The current density measured on this pseudo plateau is about 2 mA/cm². This value corresponds to a corrosion rate of about 20 mm a^{-1} (using the Faraday law for Ti → Ti^{IV}, i.e. E > −0.7 V). The decrease of current densities after the anodic peak is the consequence of a modification of the metal surface. A part of the species generated by the imposed increase of potential leads to a limitation of metal corrosion. The high value of current in this domain evidences that no anodic protection is possible on titanium. This figure also exhibits the domain of each titanium species that is present in the glass. The domains are determined from formal potentials given above.

Considering the formal potential previously determined, the intensity-potential curve of titanium in glass can be interpreted as follows:

- at the free open circuit potential (called corrosion potential), i.e. −1.4 V, titanium is oxidized to Ti^{II} ions and the main oxidant species is Si^{IV}. Furthermore, Ti^{II} is the main oxidation product from corrosion potential to about −1.0 V.
- in the −1.0 V to −0.7 V potential range, the main corrosion product is Ti^{III}. The pseudo passive plateau observed in the I=$f(E)$ curve (figure 4) indicates that the Ti_2O_3 scale is not very protective.
- for potentials less negative than −0.7 V, the oxidation of Ti leads to the formation of TiO_2.

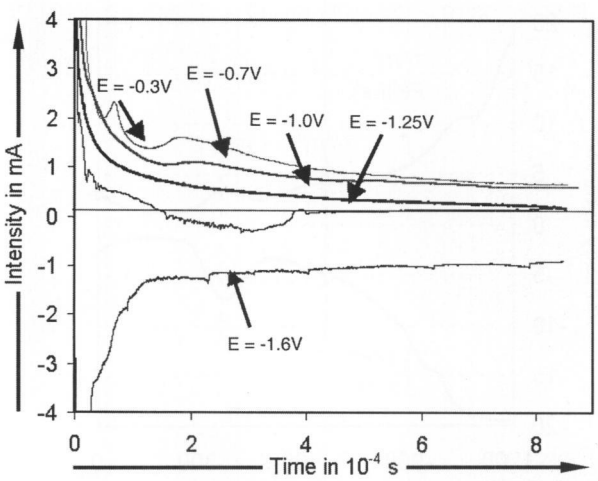

Figure 5. Current densities of the Ti rods versus time during polarization at −0.30, −0.70, −1.00, −1.25 and −1.60 V, T = 1050 °C.

4.4 Anodic and cathodic polarization of titanium rods

In order to state the corrosion mechanism of titanium in glass more precisely, four different anodic polarizations at selected potential values were realized on titanium rods for 24 h (respectively −0.30 V, −0.70 V, −1.00 V and −1.25 V). One cathodic polarization was performed on a Ti rod at −1.60 V. The intensity recordings are reported in figure 5. In every case, the intensity is stabilized after 3 h. Corresponding photomicrographs are provided in figures 6a to f. The different phases that are present at the metal/glass interface were analyzed by EPMA. The results are directly reported in the corresponding figures. The sample thicknesses that were determined yield the corrosion rate determination (figure 7). The TiO_x/silicide interfaces are irregular and a ± 5 µm error can be estimated on these measurements (the initial diameter of the Ti rod was 5.5 mm).

Figure 7 shows the corrosion rate variations as a function of the imposed potentials. The total charges are integrated from the intensity recordings for each imposed potential. These data are correlated with the corrosion rates. Attempts to reckon the corrosion rates from total charges using the Faraday law yield hazardous results. Indeed, the electrochemical reactions are complex and lead to numerous products with different densities. The product amounts are variable from one sample to another.

The sequences of titanium oxides that are formed at the metal/glass interface of Ti rods subjected to imposed potential are in good agreement with the formal potentials of Ti^{n+}/Ti^{m+} redox couples previously determined. TiO_2 is observed at −0.70 V and −0.30 V. Ti_2O_3 forms when the potential is higher than −1.00 V. When the imposed potential is lower than −1.0 V, no titanium oxide is located at the metal/glass interface, indicating that Ti^{II} species are soluble in molten glass. The titanium rods always contain oxygen in solid solution after the immersion run. As a consequence, the potential of the TiO_x formation is lower than −1.6 V.

Considering the cathodic reactions, the B^{III} reduction begins when the potential is near corrosion potential (i.e. −1.40 V), yielding TiB_2 formation. This phase was not ob-

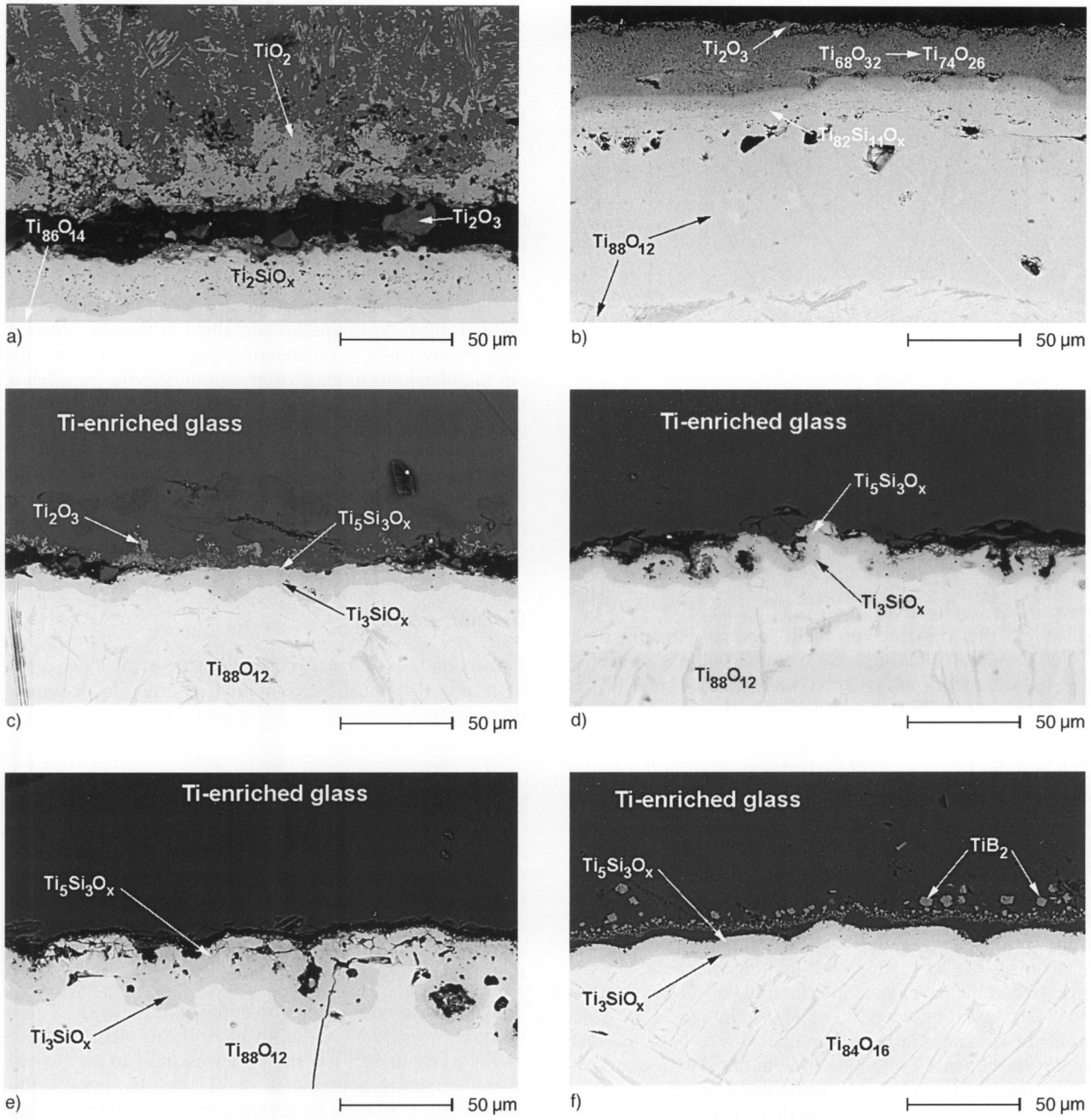

Figures 6a to f. Sections of the 24 h polarized rods presented as a function of the imposed potential on the working electrode (T = 1050 °C); imposed potentials a) −0.30 V, b) −0.70 V, c) −1.0 V, d) −1.25 V, f) −1.60 V, and e) corrosion potential.

served on the sample polarized at −1.25 V. As a consequence, the formal potential of the B^{III}/B^0 couple can be positioned at about −1.40 V. The reduction of B^{III} present in the glass was also observed in the case of Ti corrosion. The reduction of B^{III} species present in the glass must be taken into account in the case of metals or alloys whose corrosion potentials are lower than −1.4 V.

The titanium corrosion rate determined after imposing a −1.6 V potential for 24 h from thickness loss measurement is very high (60 mm a^{-1}). This is due to the dispersion of the TiB_2 grains that form a discontinuous and nonprotective layer around the titanium rod. These precipitates are oxidized when the electrical contact with the coupon is cut. This phenomenon was directly observed after a complementary experiment that consisted of imposing a −1.60 V potential to the titanium rod for 24 h and coming back to the corrosion potential during 10 min before quenching the sample. No TiB_2 layer was observed at the metal/glass interface of this sample.

The succession of the titanium silicides observed at the metal/glass interface (Ti_3Si → Ti_5Si_3) is in good agreement with the Ti−Si phase diagram [11]. When the imposed potential is lower than −1.0 V, the silicate network reduction to Si^0 is predicted by the position of the redox potentials. Indeed, the reduction wave of Si^{IV}/Si^0 begins between −1.0 and −1.1 V [2]. When the imposed potential is equal to −1.0 V, titanium silicides and Ti_2O_3 are simultaneously formed. This corresponds to the beginning of the reduction

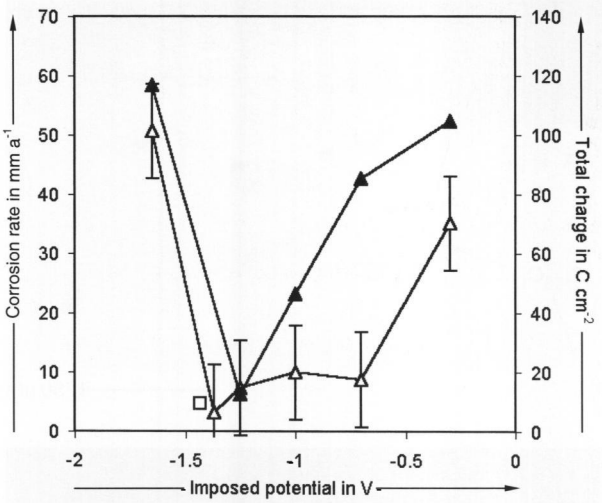

Figure 7. Plots of the corrosion rates and total charges (absolute values) as a function of the imposed potential on the Ti rod; ▲: total charges, △: corrosion rates measured without rotation, □: corrosion rates measured with rotation.

wave of Si^{IV}/Si^{0} and of the oxidation wave of Ti^{III}/Ti^{II}. However, the presence of $TiSi_x$ compounds on both −0.70 V and −0.30 V imposed potential samples is surprising. Indeed, the formal potential scale indicates that Si^{IV} is the thermodynamically stable species at these potentials.

The imposed potential experiments were carried out for 24 h in order to obtain sufficiently large grains at the metal/glass interface to achieve EPM analyses. Shorter runs would have resulted in obtaining corrosion phases too small for further analyses. Elemental composition profiles were determined in the glass from the metal/glass interface to the bulk of the glass (figures 8a to d) for each imposed potential sample. These figures show significant changes in the glass composition close to the metallic coupon up to 500 to 1000 µm in the bulk glass. The Ti content in the glass is increased at the metal/glass interface by the corrosion products' dissolution in the glass, while the Na^+ and Ca^{2+} contents are decreased in the same time. It is to be noted that no corrosion phase containing sodium or calcium is present at the metal/glass interface. Furthermore, the results given in figures 8a to d clearly indicate that the intensity of these variations is modified as a function of the imposed potential.

a) When the potential is equal to the corrosion potential, the global glass element content decrease that is observed only corresponds to the dissolution of titanium in the glass that is associated to the corrosion processes.

b) When the imposed potential is equal to −0.30 V, the titanium rod is the anode in the electrochemical system. In this case, the platinum counter electrode is the cathode of the electrochemical system, and its potential can be estimated to be about −1.2 V (the reduction of the silica network is clearly demonstrated by the formation of platinum silicides observed by SEM after the experiment). The cations that are present in the glass can migrate under the influence of the electric field existing between both electrodes. The glass surrounding the Ti rod is Na^+ and Ca^{2+} depleted (figures 8a and b). The Ca^{2+} depletion is more intense than the Na^+ depletion because of the higher charge/ionic radius ratio for Ca^{2+} than for Na^+.

c) When the imposed potential is equal to −1.60 V, the titanium rod is the cathode in the electrochemical system. The Ti rod attracts the cations. No intense Na^+ and Ca^{2+} depletion is observed in the glass surrounding the electrode. Furthermore, the glass is enriched by titanium species by the partial dissolution of the corrosion products. The charge balance in the glass is locally assumed by the decrease in the SiO_2 content.

d) When the imposed potential is in the −0.30 V to E_c range, the glass elemental variations are included in the limits described above.

These composition variations are due to the electric field assisted diffusion of species contained in the glass matrix. This phenomenon is sufficiently energetic to allow important modifications of glass composition near the metal/glass interface after 24 h run. As a consequence, this type of experiment must not be conducted for duration longer than 24 h. Otherwise, the diffusion of the cations present in the glass would yield important bulk glass modifications. Finally, the system studied would be too different from the initial one.

5. Discussion

Immersion tests and electrochemical studies yield two series of results that must be compared in order to determine their accuracy.

5.1 Corrosion rates

The corrosion rates determined from immersion tests in the G–S glass are in the same order of magnitude as those reckoned from polarization resistance measurements (a few mm a^{-1} when T=1050 °C). Di Martino et al. [2] have already extensively demonstrated the correspondence between both parameters in molten glasses.

The measured corrosion potential of Ti in the G–S glass is equal to −1.35 V. Additions of oxidizing elements (such as Zn^{II}, Fe^{II} or Fe^{III}) in the bulk glass lead to an increase in the corrosion potential of the Ti rod immersed in the glass. While it has not been experimentally determined, the corrosion potential of Ti in G–Fe and G–Zn can be estimated from the redox couple values to about −1.0 V → −0.7 V. Previous electrochemical measurements indicate that an increase in the corrosion potentials yields an increase in the corrosion rate (figure 7). The corrosion rates determined in the G–Fe and G–Zn glasses by thickness loss measurements are higher than those determined in the G–S glass (in the same duration and temperature conditions). The two data sets are consistent.

5.2 Corrosion mechanisms

The redox couples involved in the corrosion reaction can be determined from figure 2 and from the estimated or measured values of corrosion potentials. In the G–Zn glass, both Si^{IV} and Zn^{II} can corrode Ti. Zn^{II} is more oxidizing than Si^{IV} (figure 2) and the titanium rod can be oxidized up to Ti^{IV} (because of the incertitude on the relative positioning

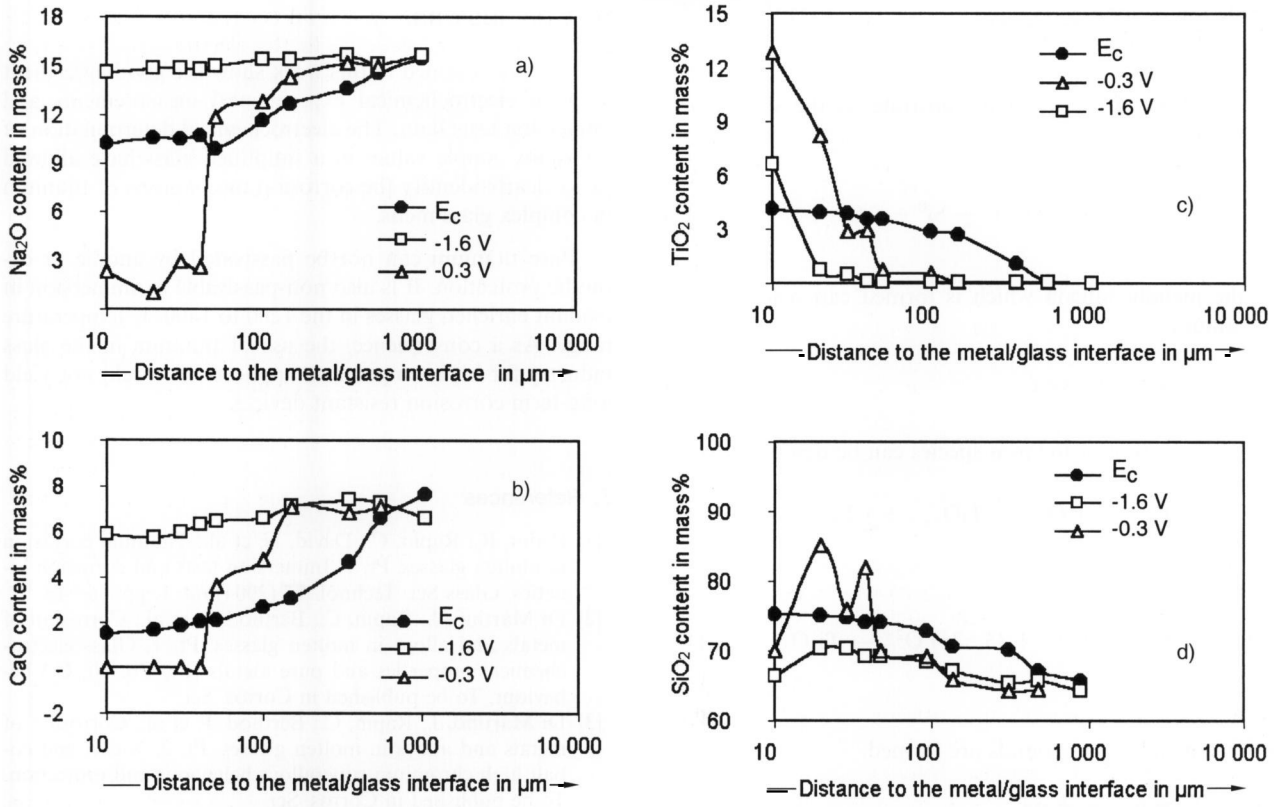

Figures 8a to d. Concentration profiles of a) Na, b) Ca, c) Ti, and d) Si in the glass as a function of the imposed potential and of the metal/glass interface distance (t = 24 h, T = 1050 °C).

of the Zn^{II}/Zn^0 and Ti^{IV}/Ti^{III} redox couples). Correlatively, Zn^{II} can be reduced to Zn^0 (gas) and Si^{IV} to Si^0. The formation of silicides is observed at the beginning of the metal/glass contact. This indicates that at the first moment of the Ti immersion in the glass, the corrosion potential of titanium is low, and the first redox reactions are the oxidation of Ti in TiO_x coupled with the reduction of Si^{IV} to Si^0. Silicon diffuses into the coupon and silicides are formed. The silicide formation yields a corrosion potential increase that corresponds to the modification of the involved redox couples. Zn^{II} present in the glass can oxidize the titanium coupon. Zn^0 bubbles grow while Ti_2O_3 or TiO_2 oxides are formed at the metal/glass interface. $TiSi_x$ are oxidized or silicon diffuses into the titanium matrix. These observations are in good agreement with the electrochemical predictions and with the metallographic cross sections of Ti immersed into the G−Zn glass [1].

The reactions that can be associated to the observed phenomenon in the G−Zn glass are:

- Oxidation of the titanium substrate by the silicate network:

$$Ti^0 + \frac{x}{2} SiO_4^{4-} \rightarrow TiO_x + \frac{x}{2} Si^0 + x O^{2-} . \quad (6)$$

- The metallic silicon which is formed can react with the titanium-oxygen solid solution:

$$3\ TiO_x + Si^0 \rightarrow Ti_3SiO_{3x} . \quad (7)$$

- The presence of bubbles indicates that a change in the redox oxidizing system occurs. It is due to the Zn^{II} reduction and Zn metal volatilization at the metal/glass interface:

$$TiO_x + y\ Zn^{2+} + y\ O^{2-} \rightarrow TiO_{x+y} + y\ Zn^0_{(gas)} \quad (8)$$

or

$$2\ TiO_x + (3-2x)\ Zn^{2+} + (3-2x)\ O^{2-} \rightarrow Ti_2O_3 + (3-2x)\ Zn^0_{(gas)} \quad (9)$$

or

$$TiO_x + (2-x)\ Zn^{2+} + (2-x)\ O^{2-} \rightarrow TiO_2 + (2-x)\ Zn^0_{(gas)} . \quad (10)$$

In the G−Fe glass, the main oxidant species are Fe^{III}, Fe^{II} and the silicate network. The expected reduction products are metallic silicon and iron, while the expected oxidation species can be Ti_2O_3 or TiO_2. The metallographic section observations indicate that silicides are formed at the first moments of the immersion of Ti in the G−Fe glass. This corresponds to the Si^{IV} reduction to Si^0 and to the oxidation of Ti to TiO_x. With continuing immersion, titanium is oxidized to Ti^{III} and Ti^{IV} while Fe^{III} is reduced to Fe^{II} and/or Fe^0. Diffusion of Si and Fe into the Ti coupon yields the formation of intermetallic compounds. These compounds, of various compositions in the Ti−Fe−Si−O phase diagram, are formed at the metal/glass interface and

inside the coupon. Consequently, the reactions that can be associated to the observed phenomenon in the G–Fe glass are:

- oxidation of the titanium substrate by the silicate network:

$$Ti^0 + \frac{x}{2} SiO_4^{4-} \rightarrow TiO_x + \frac{x}{2} Si^0 + x\, O^{2-}, \quad (11)$$

- the metallic silicon which is formed can react with titanium:

$$3\, TiO_x + Si^0 \rightarrow Ti_3SiO_{3x}, \quad (12)$$

- the reduction of the iron species can be described by:

$$TiO_x + y\, Fe^{2+} + y\, O^{2-} \rightarrow TiO_{x+y} + y\, Fe^0 \quad (13)$$

or

$$2\, TiO_x + (3-2x)\, Fe^{2+} + (3-2x)\, O^{2-} \rightarrow Ti_2O_3 + (3-2x)\, Fe^0, \quad (14)$$

- intermetallic compounds are formed:

$$TiO_x + y\, Fe^0 \rightarrow TiFe_yO_x \quad (15)$$

or

$$TiSi_zO_x + y\, Fe^0 \rightarrow TiFe_ySi_zO_x. \quad (16)$$

In both glasses, the fragmentation of the uppermost Ti_2O_3 scale can yield the formation of TiO_2 grains by further oxidation in the glass by Fe^{III}.

In the glasses containing oxidizing elements, Ti_2O_3 oxide is formed. This scale is fragmented and contains lots of faults (metallic inclusions, cracks, holes filled with glass...). This is characteristic of nonprotective corrosion products: titanium is a nonpassivable metal in glass melts. This is in good agreement with the potentiodynamic curve recorded on Ti in the G–S glass (figure 4).

As regards the corrosion rates, pure titanium can not be passivated by anodic or cathodic protection. In contrast, Ni and Co based superalloys containing 30 wt% chromium are passivable by anodic protection [3]. A characteristic corrosion rate value of a passive alloy is about 2 mm a^{-1}. The corresponding R_p value is 800 Ω cm^2. Those values are determined in the same glass composition and in the same temperature condition as those used in the present study.

Contact:

Renaud Podor
Laboratoire de Chimie du Solide Minéral
UMR 7555
Faculté des Sciences et Techniques
BP 239
F-54506 Vandoeuvre-les-Nancy
E-mail: renaud.podor@lcsm.uhp-nancy.fr

6. Conclusions

The results obtained in this work show the good agreement between electrochemical experimental measurements and immersion tests data. The electrochemical determination of the redox couple values in a simplified glass have allowed us to clearly identify the corrosion mechanisms of titanium in complex glass melts.

Pure titanium can not be passivated by anodic or cathodic protection. It is also non-passivable by immersion in oxidant enriched glasses in the 1200 to 1400 °C temperature range. As a consequence, the use of titanium in the glass industry for high temperature applications would not yield long-term corrosion resistant devices.

7. References

[1] Podor, R.; Rapin, C.; David, N. et al.: Titanium corrosion in molten glasses. Pt. 1. Immersion tests and corrosion kinetics. Glass Sci. Technol. **77** (2004) no. 1, pp. 36–43.
[2] Di Martino, J.; Rapin, C.; Berthod, P. et al.: Corrosion of metals and alloys in molten glasses. Pt. 1. Glass electrochemical properties and pure metals (Fe, Co, Ni, Cr) behaviour. To be published in Corros. Sci.
[3] Di Martino, J.; Rapin, C.; Berthod, P. et al.: Corrosion of metals and alloys in molten glasses. Pt. 2. Nickel and cobalt high chromium superalloys behaviour and protection. To be published in Corros. Sci.
[4] Baucke, F.: Electrochemical cells for the online measurements of oxygen fugacities in glass-forming melts. Glastech. Ber. **61** (1988) no. 4, pp. 87–90.
[5] Deportes, C. ; Darcy, M.: Sur une électrode de comparaison utilisable à haute température dans les sels oxygénés. Silic. ind. **26** (1961) no. 11, pp. 499–504.
[6] Von der Gönna, G.; Rüssel, C.: Redox equilibria and polyvalent elements in binary $Na_2O \cdot xSiO_2$ melts. Glastech. Ber. Glass Sci. Technol. **73** (2000) no. 4, pp. 105–110.
[7] Rüssel, C.: The electrical behaviour of some polyvalent elements in a soda-lime-silica glass melt. J. Non-Cryst. Solids **119** (1990) pp. 303–309.
[8] Claussen, O.; Rüssel, C.: Voltammetric investigations of the redox behaviour of Fe, Ni, Co and Sn doped glass melts of AR and BK7 type. Glastech. Ber. Glass Sci. Technol. **73** (2000) no. 2, pp. 33–38.
[9] Medlin, M. W.; Sienerth, K. D.; Shreiber, H. B.: Electrochemical determination of reduction potentials in glass-forming melts. J. Non-Cryst. Solids **240** (1998) pp. 193–201.
[10] Di Martino, J.; Rapin, C.; Berthod, P. et al.: Electrochemical study of metals and alloys corrosion by molten glasses. In: Proc. 15th International Corrosion Congress – Frontiers in Corrosion Science and Technology, Granada (Spain) 2002.
[11] Massalski, T. B.: Binary alloy phase diagrams. Metals Park, OH: American Society for Metals, 1990.

E204P006